Astron. Astrophys. Suppl. Ser. 92, 349-363 (1992)

ASTRONOMY & ASTROPHYSICS
SUPPLEMENT SERIES

*Astron. Astrophys. Suppl. Ser.* **92**, 349-363 (1992)



# Heliosphere instrument for spectra, composition and anisotropy at low energies

L. J. Lanzerotti[1], R. E. Gold[2], K. A. Anderson[3], T. P. Armstrong[4], R. P. Lin[3], S. M. Krimigis[2], M. Pick[5], E. C. Roelof[2], E. T. Sarris[6], G. M. Simnett[7] and W. E. Frain[2]

[1] AT&T Bell Laboratories, Murray Hill, New Jersey, 07974, USA
[2] Applied Physics Laboratory, The Johns Hopkins University, Laurel, Maryland, USA
[3] Space Sciences Laboratory, University of California, Berkeley, USA
[4] Department of Physics, University of Kansas, Lawrence, USA
[5] Observatoire de Paris, Meudon, France
[6] University of Thrace, Xanthi, Greece
[7] University of Birmingham, UK

*Received April 24; accepted August 19,1991*

**Abstract.** — The Heliosphere Instrument for Spectra, Composition, and Anisotropy at Low Energies (HI-SCALE) is designed to make measurements of interplanetary ions and electrons throughout the entire Ulysses mission. The ions ($E_i \gtrsim 50$ keV) and electrons ($E_e \gtrsim 30$ keV) are identified uniquely and detected by five separate solid-state detector telescopes that are oriented to give nearly complete pitch-angle coverage (i.e., coverage of essentially $4\pi$ ster) from the spinning spacecraft. Ion elemental abundances are determined by a $\Delta E$ vs $E$ telescope using a thin (5 $\mu$m) front solid state detector element in a three-element telescope. Experiment operation is controlled by a microprocessor-based data system. Inflight calibration is provided by radioactive sources mounted on telescope covers which can be closed for calibration purposes and for radiation protection during the course of the mission. Ion and electron spectral information is determined using both broad-energy-range rate channels and a 32 channel pulse-height analyser (channels spaced logarithmically) for more detailed spectra. The instrument weighs 5.775 kg and uses 4.0 W of power. Some initial in-ecliptic measurements are presented which demonstrate the features of the instrument.

**Key words:** Sun: activity - cosmic rays - flares, interplanetary medium.

## 1. Scientific objectives.

The HI-SCALE experiment (in ESA engineering documents, the experiment is identified by the three-letter acronym LAN) is designed to make significant advances toward understanding physical processes involved in the solar control of low-energy ions and electrons in the heliosphere. The Ulysses mission provides the opportunity to carry out such investigations in regions of the heliosphere never before studied. The extraordinarily fruitful scientific return expected from such a mission has been discussed since the earliest days of spaceflight (Simpson *et al.*, 1959, Fisk & Axford, 1976), and more recent observational and theoretical considerations have enabled the objectives defined in the planning stages of Ulysses to be updated and refined (Wenzel, 1980). These have largely remained unchanged during the lengthy delays in the program.

*Send offprint requests to*: L. J. Lanzerotti.

The highest priority scientific objectives for the HI-SCALE experiment arise specifically from the unique, exploratory nature of the Ulysses mission. The objectives (discussed below) have been refined by taking into explicit consideration the most current theoretical and modelling efforts in heliospheric physics. The launch of Ulysses in October 1990 occurred during the peak of solar activity in solar cycle 22. Ulysses, after Jupiter encounter in February 1992, will ascend out of the ecliptic plane during the declining phase of the cycle. HI-SCALE will make significant contributions to Ulysses science during this interval and during the polar passes, which will occur near solar minimum.

There are a number of key heliospheric scientific objectives for which HI-SCALE has been designed. However, the instrument is a versatile one that can also make measurements over a broad dynamic range in energy and intensity, essential requirements in an exploratory mission into unknown regions. The heliosphere objectives include the following (the few included references have intention-

ally been restricted to some of the contributions in these areas by members of the HI-SCALE team).

— Low energy solar particle fluxes will be used as probes of the morphological changes in coronal and interplanetary magnetic field structures as a function of heliolatitude. The corona controls, in important but little-understood ways, the release of solar-flare particles into the heliosphere. On the other hand, the large-scale structure of the interplanetary magnetic field controls the propagation, and therefore the later history, of a solar particle event. Plasma disturbances (e.g., interplanetary shocks) associated with the flare itself (as well as those associated with earlier flares) violently distort the interplanetary magnetic field. It is possible to "label" interplanetary magnetic field lines (even those that are strongly deformed by the flare plasma ejecta) by the helio-longitude and latitude of their connection to the high solar corona. Figure 1 illustrates the intensity/time profile of solar-flare particles referenced to fixed heliolongitudes as derived from measurements made by five well-separated spacecraft spaced azimuthally in the ecliptic plane at 1 A.U. (Reinhard, Roelof & Gold, 1986). One day after the flare, the maximum particle flux systematically shifts, to longitudes nearly 180° from the flare longitude (60°). As in most large events, coronal effects appear to be dominant during the first day after the flare, while the outer heliosphere plays the dominant role in sustaining the monotonic heliolongitude gradient of the fluxes late in the events. During the many-day decay phase of large solar events, the spatial gradient of particle fluxes along field lines is remarkably small over many A.U. (Roelof, 1986), making it possible to compare directly the particle fluxes measured at Ulysses to those observed by monitors near Earth. The HI-SCALE measurements will be important in elucidating the physical mechanisms by which coronal structures are extended from the Sun into the outer heliosphere, not only near the ecliptic, but at all latitudes.

— Solar-flare processes will be studied and the physical conditions in flares will be modeled using the measurements of both relativistic and nonrelativistic energy electrons and nonrelativistic energy ions. Comparisons of radioheliograph measurements of solar type-III radio bursts with coronal structures imaged in white light on the Solar Maximum Mission indicate that there is a strong latitude dependence in the escape of such particles. (Trottet *et al.*, 1982).

— Increased insight into the basic astrophysical question of solar elemental abundances will be achieved by means of measurements of the chemical (atomic) composition of low-energy nuclei emitted from the Sun in the active region band and at high heliolatitudes. Comparisons will be made with similar measurements carried out in the ecliptic plane (Zwickl *et al.*,1978).

— The parameters of low-energy solar particle propagation in interplanetary space will be determined using measurements of the particle anisotropy and composition as functions of heliographic latitude. Of particular interest will be the study of particle propagation in the vicinity of the neutral sheet in the interplanetary magnetic field (Smith, 1990).

— Correlations of non-relativistic electron events with on-board Ulysses radio measurements (Lin *et al.*, 1981) will provide quantitative physical parameters of outward-propagating wave-particle interactions at different latitudes in the heliolatitude-dependent interplanetary
plasma.

— Changes in particle energy distributions will be measured and the physical processes in the interplanetary medium that cause them will be identified. Particular emphasis will be placed on modelling the changes produced by shock, stochastic, and other possible mechanisms of particle acceleration as the Ulysses spacecraft moves away from the ecliptic plane. For example, low-energy particles can be energized in association with interplanetary shock waves produced by solar flares or by shock pairs associated with co-rotating interaction regions (Pesses, Decker & Armstrong, 1982, Sarris & Krimigis, 1985, Decker & Vlahos, 1986, Decker, 1985). The anticipated particle intensity versus time signatures for forward-reverse shock pairs observed north of, south of, and on the ecliptic are shown in Figure 2 for the case of negative interplanetary field polarity (the results will be reversed north to south for positive polarity) (Sarris, 1983). Analyses of data from the two Voyager spacecraft in the outer heliosphere has shown clearly that at heliolatitudes greater than $\sim 20°$, the shock-produced particle enhancements are significantly fewer in number and tend to be less intense than for those events measured in the ecliptic plane (Gold *et al.*, 1988). Shown in Figure 3 are comparisons of the average energy spectra of several shock-associated events observed on the Voyager spacecraft at equatorial and high heliospheric latitudes (Gold *et al.*, 1988).

— The 'quiet-time' low-energy particle populations in the interplanetary medium will be measured, and the possible separation of the solar, galactic, and planetary magnetosphere components will be made by their different heliolatitude variations (Krimigis *et al.*, 1977).

— Measurements of the temporal and spatial variations in low-energy particle intensities and compositions in the vicinity of the Jovian magnetosphere will be made.

— The new knowledge gained from HI-SCALE and Ulysses investigations of the global dynamics and structure of the heliosphere will be used to define in a more quantitative way the influences of solar activity on the terrestrial environment and its technological systems (Lanzerotti, 1979; Medford *et al.*, 1989).

## 2. The instrument.

The HI-SCALE experiment consists of five apertures in two separate telescope assemblies that are mounted by means of individual stub arms on a box containing all of the instrument electronics. The entire instrument is mounted on one corner of the Ulysses spacecraft to give unimpeded fields of view to the telescopes.

The HI-SCALE instrument and one of its electronics circuit boards are shown in Figures 4a,b. The entire instrument weighs 5.775 kg and consumes 4.0 W of electrical power. An additional 7.5 W of power are available for heaters used in the telescopes and for the log amplifiers (see below) as well as for the cover closure mechanisms (see below). Further details of the instrument, as well as data processing information, are continued in a technical report (Armstrong *et al.*, 1991).

### 2.1. Sensor system.

The measurements required to fulfill the heliospheric science objectives cannot be made with a single charged-particle sensor. To attain the lowest energy of response over a wide variety of particle species with high sensitivity geometrical factors and angular resolution, HI-SCALE utilizes three distinct silicon solid-state detector systems. These are Low-Energy Magnetic/Foil Spectrometers (LEMS/LEFS) and the Composition Aperture (CA; sometimes referred to in the Ulysses project as the "WART"). The LEMS/LEFS systems provide pulse-height-analyzed single-detector measurements with active anticoincidence. The CA system uses a multiparameter detection technique to provide measurements of ion composition in an energy range similar to those of LEMS/LEFS. The foil thickness, detector thicknesses, and electronic thresholds were selected to enable the separation of low energy electron and ion fluxes at high sensitivity by comparing detector responses.

The five separate detector systems are contained within two mechanical telescope structures, as shown in Figure 5. The individual telescopes are referred to as LEFS 60, LEFS 150, LEMS 30, LEMS 120 and CA 60, where the number indicates the inclination of the telescope axis with respect to the spacecraft spin axis.

The MF, M′ F′, and BC detector pairs (Tab. 1) are identical (for ease of replacement pre-flight); each consists of two equal 200 $\mu$m thick, totally depleted silicon surface barrier detectors. The D detector is a thin (5 $\mu$m) silicon detector of the epitaxial type.

The opening angles and spin-axis orientations of the telescopes are shown schematically in Figure 6a. The orientations of the telescope axes are such that there is nearly a complete $4\pi$ coverage of the unit sphere during one complete spacecraft spin. This is shown schematically in Fig. 6b. The detector opening apertures are shown, on the vertical axis, with the appropriate values of their polar angles measured from the spacecraft spin vector and as a function, on the horizontal axis, of their location, at a given instant, relative to the spin plane clock angle measured from the spacecraft $x$-axis.

In the LEMS 30 and 120 telescopes, electrons with energies below ~300 keV are swept away from detectors M and M′ by a rare-earth magnet. The geometric factor for the ions measured by detectors M and M′ is ~ 0.48 cm$^2$sr. The ion energy channels are listed in Table 1 (the energy channels for both LEMS telescopes are essentially identical).

In the LEFS 60 and LEFS 120 telescopes, a thin (~0.35 mg cm$^{-2}$) aluminized parylene foil prevents ions ($\lesssim$350 keV) from reaching the F and F′ detector, while electrons ($\gtrsim$30 keV) can penetrate the foil with little energy loss. The logic and energy channels for both LEFS telescopes are listed in Table 2. Both telescopes also have a geometrical factor of ~0.48 cm$^2$ sr.

In the LEMS 30 telescope, the magnetically-deflected electrons are counted by a separate detector B, with a geometrical factor of ~0.05 cm$^2$sr. The electron energy channels for B with their defining logic are shown in Table 1. Two-dimensional particle ray tracing in a magnetic field similar to that of LEMS 30 is shown in Figure 7. Such two-dimensional (and similar three-dimensional) computer ray-tracing studies have been used together with calibration data obtained with a particle accelerator to determine the effective field-of-view of the telescope aperture.

The CA telescope uses detectors D and C (Fig. 5) as an ($\Delta E$ vs $E$) telescope, with the B detector operating in anticoincidence. The geometrical factor for the DCB combination is 0.24 cm$^2$sr. The logic and discrete energy channels for the CA telescope are shown in Table 3.

Information from the discrete ion composition channels listed in Table 3 is used in a priority scheme to identify those individual particle events whose energy loss signals in detectors D and C are to be pulse-height-analysed (see below) and included in the telemetry data stream.

A rotating four-level priority scheme, shown in Table 4, is used to balance the CA system response to light and heavy ion species.

The priority scheme uses the species group analyzed in the immediate previous event in a given sector to

establish the relative priorities among the four species groups for the current sector. Thus, if there were an iron-group event analyzed in the immediate previous spin, the fourth column of Table 4 would be operative and shows that the priority order for analysis, from the highest to the lowest priority, would be an event in the oxygen group, the iron group, helium, and protons. Thus, the priority scheme insures that a large number of relatively "rare" ion species will be presented for analysis.

The pulse-height-analyser system is also used to make detailed energy spectral measurements of the electron and ion fluxes that are detected by the LEMS and LEFS telescopes.

In addition to the discrete telescope logic channels that are listed Tables 1-3, the singles counting rates in the individual detectors are monitored and telemetered in a multiplexed mode (Tab. 2). These rates are used as engineering monitors of the instrument performance. These rates can also be used, if required, to make pulse-pileup corrections to the coincidence rates.

### 2.2. ELECTRONICS SYSTEMS.

An overall HI-SCALE system electronics block diagram is shown in Figure 8.

#### 2.2.1. *Analog electronics.*

The signals from the individual detectors are fed to charge-sensitive preamplifiers, linear shaping amplifiers and then to discriminators. The analog electronics are largely of hybrid construction. In addition to the preamplifer, amplifier, and discriminator circuits these hybrid circuits also include logarithmic amplifiers, accumulators, one-shots, peak detectors, power controllers and interface modules required for the pulse-height-analyzer system.

The HI-SCALE log amplifiers, used in the CA system and with the pulse-height-analyzed signals from the F and M detectors, provide an accurate logarithmic response over a $> 10^3$ dynamic range, with calibration curves available over a $> 10^4$ range. The design uses temperature compensation and temperature stabilization by heaters to ensure accurate performance throughout the mission.

The count rate logic (used to define the energy channels listed in Tab. 1-3) employs relatively simple, single-detector, differential energy windows. The CA ion composition rate channels use slanted discriminators to define the species group channels defined in Table 3.

#### 2.2.2. *Data system.*

The HI-SCALE experiment is under the overall control of a radiation-hardened 1802 microprocessor and its associated peripheral devices. The system uses 6K ROM and 3K RAM memory. If there should be a partial failure, provision is made for recovery by loading a substitute program into RAM and then using this in the normal program execution sequence.

The science data are collected and sector-organized (see below) over a cycle of ten spacecraft spin periods (~120s), or a multiple thereof, then output (with status information) into the spacecraft telemetry stream. The science data are synchronized so that one cycle is output during four consecutive spacecraft formats.

The Ulysses telemetry system accepts data from HI-SCALE in four bit-rate modes. The experiment data output format is identical in each bit-rate mode. During the fastest telemetry mode, the HI-SCALE bit rate is 160 bit/s. The spacecraft will accept a complete data format in 128s, with an experiment accumulating data over 10 spin periods (~120s). In the slowest telemetry mode, the complete data format is output in 1024s, and the experiment accumulates data over 80 spin periods.

Angular distributions of the detected particles are obtained by dividing each complete spin into four or eight sectors of equal duration. Two separate sectoring modes, selected by command, are available. During the sun sectoring mode, each spin is defined to begin some fraction of a spin after the Sun-spacecraft meridian is crossed. If, for some reason, the interval between Sun crossings is outside some fixed limits, a time-sectoring mode is automatically selected. A pseudo-sector is created by command and accumulations then occur in 'sectors' of this determined period. In either sectoring mode, the ground data processing will relate the nearly complete coverage of the unit sphere (see Fig. 6b) to pitch angle relationships with the interplanetary magnetic-field measurements made by the Ulysses magnetometer experiment.

### 2.3. ANGULAR DISTRIBUTIONS.

An important consideration for charged-particle studies on Ulysses is the fact that the direction of the interplanetary magnetic field (which controls low-energy-particle propagation) changes with respect to the spacecraft spin axis throughout the mission. This is particularly true, and of key importance, for the prime out-of-ecliptic mission phase, after Jupiter encounter. Therefore, many diverse and antithetical requirements are placed on detector orientation if it is desired to make measurements over a wide range of pitch angles throughout the mission. The particular orientations of the HI-SCALE detector telescopes with respect to the Ulysses spacecraft spin axis (as described in the previous section) have been chosen primarily as a result of this consideration.

The solar-direction coverage of the LEMS 30 sensor is shown in Figure 9 together with the full range of pitch-angles swept by the centers of the combined LAN 2A and

LAN 2B telescopes (see Fig. 5) during the course of the mission following Jupiter encounter. These coverages are determined for the nominal Archimedean spiral direction of the interplanetary field. (As was shown in Fig. 6b, the orientations of the LEMS and LEFS telescopes are such as to provide essentially complete angular coverage over $4\pi$ steradians throughout the prime phase of the mission.)

## 3. Calibration.

Because of the length of the mission, it is important to have good ground-based calibration data to characterize the instrument pre-flight. An inflight calibration capability is also a necessity.

### 3.1. PREFLIGHT CALIBRATION.

A broad characterization of the instrument response to accelerated beams of ions and electrons has been carried out in order to ensure proper basic functioning of the instrument. Such characterization has been performed for both the engineering and the flight units. The electron and ion calibrations of the engineering unit have been carried out at the particle accelerator facility at Goddard Space Flight Center. Calibrations of the CA with ion beams of various charges were carried out at Rutgers University using the tandem Van de Graaff accelerator formerly at that location.

Figure 10a shows the energy-loss matrix entries for a calibration run at Rutgers with various ion species. Excellent separation of the ion tracks is clearly evident.

Contours of equal detection efficiency, across the telescope aperture, are shown in Figure 10b for 100 keV electrons counted in detector B (Tab. 1). The precise configuration of such contours is a function of electron energy and is determined for different energies both by electron calibration and by computer ray tracing.

### 3.2. INFLIGHT CALIBRATION.

Calibrations of the LEMS and CA portion of the instrument are provided in flight by the use of radioactive sources rigidly fixed to the inside of the three telescope covers. Upon command, the covers can be closed using thermally-driven bi-metallic springs attached to each cover. The telescopes will then count the source emissions. Removal of the power from the bi-metal heaters cause the covers to open slowly and completely. This feature was tested following launch and worked nominally.

The alpha particle-emitting calibration sources included on the covers are $^{241}$Am for the LEMS and $^{244}$Cm and $^{148}$Gd for the CA. The $^{241}$Am and $^{244}$Cm sources are $1\mu$Curie, and the $^{148}$Gd source is $0.1\mu$Curie.

## 4. In flight performance.

Following Ulysses launch on 6 October 1990, the covers of the HI-SCALE instrument were deployed on 3 November and the instrument was turned on for operation on 14 November. Operation since turn-on has been nominal, with all elements of the instrument system performing as designed, tested, and calibrated.

### 4.1. ION AND ELECTRON SPECTRA.

Shown in Figure 11 are time-intensity spectrogram displays of ion fluxes measured during the onset of a small particle enhancement on days 356-357, 1990. These spectrograms are generated using the measurements obtained in the 8 rate channel accumulators (see Fig. 8). The spectrograms were plotted using data obtained from the Ulysses Project QEDR's (Quick-look Experimental Data Records). The white vertical stripes indicate that data at those times were not available when the QEDR's were generated; such data are usually not missing and so the gaps in the data coverage will generally be filled in when the final data records are distributed by the Project. The intense "fluxes" in the M ion channels at the lowest energies correspond to the response of that instrument to sunlight. The spectrograms show evidence for some initial bursts of particles (day 356, hour 08 and from about 12 to 18UT) prior to the onset of the full intensity enhancements at about 00UT on day 357 (see also Fig. 13 below). Ignoring the sun signal in the M ion channels, it is qualitatively apparent that the spectra all decrease monotonically with increasing energy. (The three rows of zero value numbers at the bottom of the plot are for the inclusion of magnetic field values from the Ulysses magnetometer when they are available.)

Detailed energy spectra for the four channels of Figure 11 are plotted in Figure 12. Here, the spectra for the one hour interval from 0700-0800 on day 356 are shown using the high energy-spectral resolution capabilities of the 32 channel spectral analyzer (see Fig. 8). The error bars correspond to counting statistics. The time interval of these encompasses a portion of one of the particle bursts noted above in Figure 11. (The spectrum accumulator has 32 logarithmically-spaced channels with electronic passbands between 30 keV and 5.5 MeV. The passbands and electronics are different from those that form the LEMS channels (Tab. 1), but both subsystems count the same particles.)

Figure 13 shows time-intensity plots of electron and ion fluxes in several different energy channels in order to illustrate the low energy response of HI-SCALE. These energy channels are from the spectrum analyzer and cover the same two day interval as that in Figure 11. Panels *a,b* show the 30-50 keV electrons from LEFS60 and LEFS150, respectively; panel *c* shows the 30-50 keV protons from

LEMS120; panel *d* shows the 90-165 keV protons from LEMS30. All of the data in each of the panels is averaged over a complete spacecraft spin.

The ion spectra are plotted as a function of angular distribution in Figure 14 for the same one hour interval as the spectra of Figure 12. The 0° position is aligned with the $x$-axis of the spacecraft. Again the intense fluxes in the M channel in the 0° direction are due to sunlight. While these angular distributions are shown here primarily to demonstrate the capabilities of the instrument and the analysis software, it is evident that the particle bursts at this time are quite anisotropic.

### 4.2. ION COMPOSITION.

A large solar particle event was measured by HI-SCALE in March 1991. This event provides an excellent opportunity to "calibrate" the instrument in a flare event which contains particles covering a wide energy range and many atomic species. Shown in Figure 15 is a plot of the ion abundances as determined by the CA system (detectors C and D) for the first half day of 26 March (day 85). The tracks for the identified species are clearly visible down to the lowest energies measured in the C detector (<1MeV). The excellence with which the tracks are distinctly visible to such low energies in this $\Delta E \times E$ system is a result of the uniformity of the thickness across its area of the thin (D) detector used in the telescope.

It is not practical to provide more detailed results than those contained in this section in a paper devoted primarily to the characteristics of the HI-SCALE instrument.

**Acknowledgements.**

We thank many people at UC Berkeley and APL/JHU for design and engineering efforts. At Berkeley, R. Weitzmann and R. Campbell contributed to the telescope and detector designs, configurations and fabrication. At APL/JHU, electronic design and testing was accomplished by S. Gary, C. Tielens, D. Fort, A. Lew, S. Williams, D. Guynn and P. Schwartz; mechanical design and thermal engineering was carried out by J. Mueller and C. Wingate while R. Thompson was responsible for mechanical assembly. B. Northrup, K. Blankenship and L. Staub spent countless hours shepherding various facets of the program. We thank J. Dassoulas and B. Tossman for managing the program in its early development phase. E. Hawkins and E. Keath contributed instrument checkout characterizations and calibrations, assisted in the calibrations by J. Kohl. C. Maclennan of BTL provided magnet ray tracings. Organization of the data reduction procedures, and preparation of software for data reduction, evaluation, and analysis has been skillfully led by L. Suther of APL/JHU, with major contributions made by J. Townsend of APL/JHU, H. Choo and J. Manweiler of the University of Kansas, R. Williams and D. Curtis of UCB, and J. Tappin of the University of Birmingham. We acknowledge CNES (Centre National d'Etudes Spatiales) who will provide microfiche plots of data from the HI-SCALE experiment and from the Nancay radioheliograph. We thank S. Brown of the Goddard Space Flight Center and the staff of the Rutgers Nuclear Physics Laboratory for advice and assistance with calibrations. The work on HI-SCALE at APL/JHU has been supported by NASA under Task I of Contract N00039-89-C-0001 between The Johns Hopkins University and the Department of the Navy, and by subcontract at the University of Kansas and the University of California.

**References**

Armstrong T.P., Hawkins S.E., Shelley G. 1991, HI-SCALE Data Analysis Handbook, JHU Applied Physics Laboratory, preprint (in preparation)
Decker R.B., Vlahos L. 1986, ApJ 306, 710
Decker R.B. 1985, ApJ 324, 566
Fisk L.A., Axford W.I. (eds) 1976, Proc. Symp. Study of the Sun and Interplanetary Medium in Three Dimensions, NASA/Goddard Space Flight Center, X-660-76-53
Gold R.E., Decker R.B., Krimigis S.M., Lanzerotti L.J., Maclennan C.G. 1988, J. Geophys. Res. 93, 991
Krimigis S.M., Zwickl R.D., Kohl J.W., Armstrong T.P. 1977, Proc. 15th Int. Cosmic Ray Conf., Plovdiv, 5, 280
Lanzerotti L.J. 1979, J. Atmos. Terr. Phys., 41, 787
Medford L.V.,Lanzerotti L.J.,Kraus J.S.,Maclennan C.G. 1989, Geophys. Res. Lett. 16, 1145
Lin R.P.,Potter D.W., Gurnett D.A., Scarf,F.L. 1981, ApJ 251, 364
Pesses M.E., Decker R.B., Armstrong,T.P. 1982, Space Science Rev. 32, 185
Reinhard R., Roelof E.C., Gold R.E. 1986, in The Sun and the Heliosphere in Three Dimensions, R.G. Marsden Ed., D. Reidel (Dordrecht), 297
Roelof E.C. 1986, in The Sun and the Heliosphere in Three Dimensions, R.G. Marsden Ed., D.Reidel (Dordrecht), 331
Sarris E.T., Krimigis S.M. 1985, ApJ 298, 676.
Sarris E.T. 1983, Proc. 8th Europ. Cosmic Ray Conf., Iucci N., Storini M., Cecchini S. Massaro F. Eds., 17
Simpson J.A., Rossi B., Hibbs A.R., Jastrow R., Whipple F.L., Gold T., Parker E., Christofilos N., VanAllen J.A. 1959, J. Geophys. Res., 64, 1691
Smith E.J. 1990, J. Geophys. Res. 95, 18731
Trottet G., Pick M., House L., Illing R., Sawyer C., Wagner W. 1982, A&A 111, 306
Wenzel K.-P. 1980, Phil. Trans. R. Soc., A297, 519
Zwickl R.D., Roelof E.C., Gold R.E., Krimigis S.M., Armstrong T.P. 1978, ApJ 225, 281

TABLE 1. *LEMS detector systems.*

| | Channel | Logic | Passband[a] | Sectors | Accum. time(s) @ 1024 bit/s |
|---|---|---|---|---|---|
| LEMS 30[b] | P1 | M1 $\overline{M2}$ $\overline{F}$ | 50-73 keV ions | 4[b], 8[c] | 3[b], 1.5[c] |
| (M,F) | P2 | M2 $\overline{M3}$ $\overline{F}$ | 73-112 keV ions | 4[b], 8[c] | 3[b], 1.5[c] |
| LEMS 120[c] | P3 | M3 $\overline{M4}$ $\overline{F}$ | 112-180 keV ions | 4[b], 8[c] | 3[b], 1.5[c] |
| (M′,F′) | P4 | M4 $\overline{M5}$ $\overline{F}$ | 180-310 keV ions | 4[b], 8[c] | 3[b], 1.5[c] |
| | P5 | M5 $\overline{M6}$ $\overline{F}$ | 310-550 keV ions | 4[b], 8[c] | 6[b], 3[c] |
| ~ 0.48 cm$^2$ sr | P6 | M6 $\overline{M7}$ $\overline{F}$ | 550-1500 keV ions | 4[b], 8[c] | 6[b], 3[c] |
| | P7 | M7 $\overline{M8}$ $\overline{F}$ | 1.0-1.8 MeV ions | 4[b], 8[c] | 6[b], 3[c] |
| | P8 | M8 $\overline{F}$ | 1.5-5.0 MeV ions | 4[b], 8[c] | 6[b], 3[c] |
| LEMS 30 | DE1 | B1a $\overline{B2}$ $\overline{C}$ | 30-50 keV electrons | 4 | 6 |
| (B,C) | | B1b $\overline{B2}$ $\overline{C}$ | 40-50 keV electrons | 4 | 6 |
| ~ 0.05 cm$^2$ sr | DE2 | B2 $\overline{B3}$ $\overline{C}$ | 50-90 keV electrons | 4 | 6 |
| | DE3 | B3 $\overline{B4}$ $\overline{C}$ | 90-165 keV electrons | 4 | 6 |
| | DE4 | B4 $\overline{B5}$ $\overline{C}$ | 165-300 keV electrons | 4 | 6 |

[a] The passbands given here are provisional and subject to refinement as in-flight calibrations are completed.
[b] Sectors and accumulation times designated with *b* are associated with the LEMS 30 system.
[c] Sectors and accumulation times designated with *c* are associated with the LEMS 120 system.

TABLE 2. *LEFS detector systems.*

| | Channel | Logic | Passband[a] | Sectors | Accum. time(s) @ 1024 bit/s |
|---|---|---|---|---|---|
| LEFS 150[b] | E1 | F1 $\overline{F2}$ $\overline{M}$ | 30-50 keV electrons | 4[b], 8[c] | 3[b], 1.5[c] |
| (M, F) | E2 | F2 $\overline{F3}$ $\overline{M}$ | 50-90 keV electrons | 4[b], 8[c] | 3[b], 1.5[c] |
| LEFS 60[c] | E3 | F3 $\overline{F4}$ $\overline{M}$ | 90-165 keV electrons | 4[b], 8[c] | 3[b], 1.5[c] |
| (M′, F′) | E4 | F4 $\overline{F5}$ $\overline{M}$ | 165-300 keV electrons | 4[b], 8[c] | 3[b], 1.5[c] |
| | FP5 | F5 $\overline{F6}$ $\overline{M}$ | 300-550 keV ions | 4[b], 8[c] | 6[b], 3[c] |
| ~ 0.48 cm$^2$ sr | FP6 | F6 $\overline{F7}$ $\overline{M}$ | 550-1.0 MeV ions | 4[b], 8[c] | 6[b], 3[c] |
| | FP7 | F7 $\overline{M}$ | 1.0-5.0 MeV ions | 4[b], 8[c] | 6[b], 3[c] |
| Singles | S1 | Det. B,C,D | | | 12 |
| | S2 | Det. M,F,M′,F′ | | | 12 |

[a] See Table 1 footnote.
[b] Sectors and accumulation times designated with *b* are associated with the LEFS 150 system.
[c] Sectors and accumulation times designated with *c* are associated with the LEFS 60 system.

TABLE 3. *Ion composition.*

| | Channel | Logic | Passband[a] | Sectors | Accum. time(s) @ 1024 bit/s |
|---|---|---|---|---|---|
| CA 60[b] | W1 | C1 D1 $\overline{C2}$ $\overline{D2}$ | 0.35-1.0 MeV protons | 8 | 3 |
| | W2 | C2 D1 $\overline{D4}$ $\overline{D2}$ $\overline{S1}$ | 1.0-2.0 MeV protons | 8 | 3 |
| | W3 | C1(D2 + S1) $\overline{C3}$ $\overline{D3}$ | 0.35-1.0 MeV/nuc. He | 8 | 3 |
| | W4 | C3 D1 S1 $\overline{C4}$ $\overline{D3}$ | 1.0-5.0 MeV/nuc. He | 8 | 3 |
| | W5 | C2 D3 $\overline{C4}$ $\overline{D4}$ | ~ 0.3-1.7 MeV/nuc. C,N,O | 8 | 3 |
| | W6 | C4 D2 S2 $\overline{D4}$ $\overline{S3}$ | ~ 1.7-10 MeV/nuc. Fe | 8 | 3 |
| | W7 | C2 D4 $\overline{C4}$ | ~0.2-1.0 MeV/nuc. Fe | 8 | 3 |
| | W8 | C4 D3 S3 | ~1.0-15 MeV/nuc. Fe | 8 | 3 |
| | Z2 | | $\gtrsim$0.5 MeV, Z$\geq$2 | 4 | 6 |
| | Z2A | | $\gtrsim$10.0 MeV, Z$\geq$14 | 4 | 6 |
| | Z3 | | $\gtrsim$2.8 MeV, Z$\geq$6 | 4 | 6 |
| | Z4 | | $\gtrsim$9.0 MeV, Z$\geq$10 | 4 | 6 |

[a] See Table 1 footnote.
[b] Geometrical factor ~0.24 cm$^2$ sr

TABLE 4. *Rotating priority scheme.*

| | Species Group of Previous Event | | | |
|---|---|---|---|---|
| | H | He | O | Fe |
| Highest | Fe | H | He | O |
| Priority for Current Event | O | Fe | Fe | Fe |
| | He | O | O | He |
| Lowest | H | He | H | H |

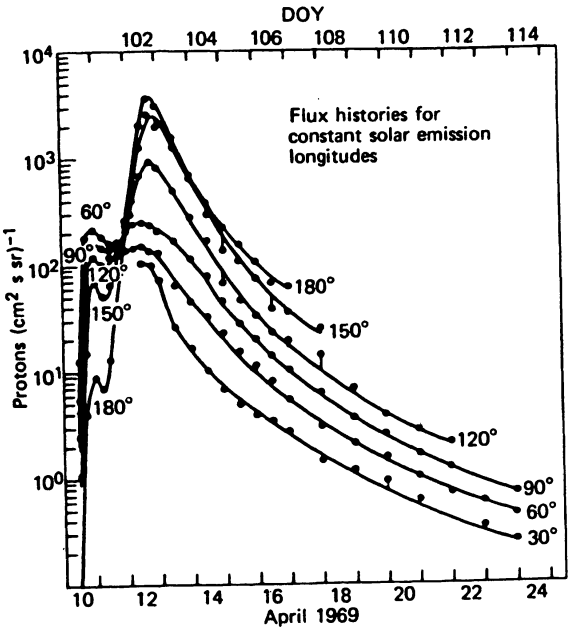


FIGURE 1. Intensity/time profiles for solar-flare particles, referenced to fixed heliolongitudes, as derived from measurements made by five spacecraft separated in azimuth in the ecliptic plane.

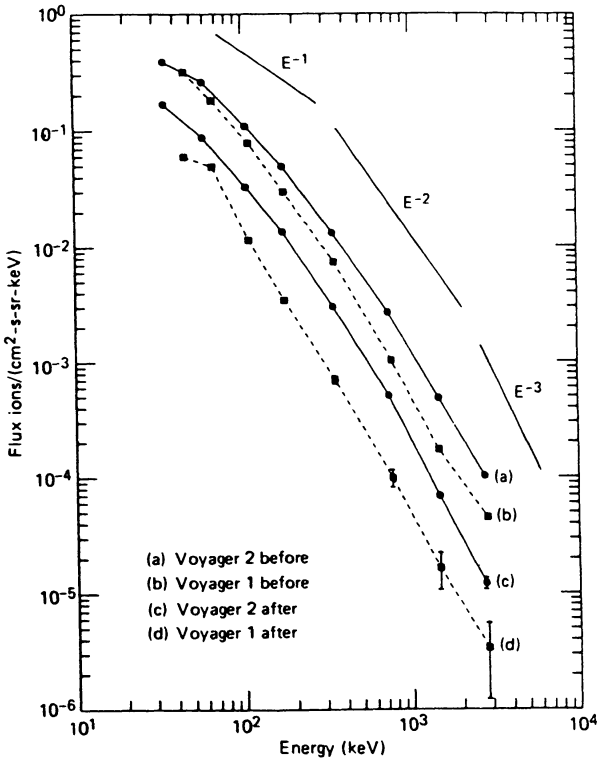


FIGURE 3. Energy spectra of interplanetary ion events associated with shocks measured on the two Voyager spacecraft (Voyager 2 in the ecliptic, Voyager 1 above the ecliptic) both before and following a large interplanetary ion flux decrease in early 1985: (a) The spectrum derived from the average of the eight largest shock-associated events observed by Voyager 2 during 1984 and 1985, prior to the large flux decrease. (b) A similar average spectrum observed by Voyager 1 before the flux decrease. (c) The average spectrum derived from the five largest events observed by Voyager 2 after the flux increase in early 1985. (d) The average spectrum of the five largest events at Voyager 1 after the decrease.

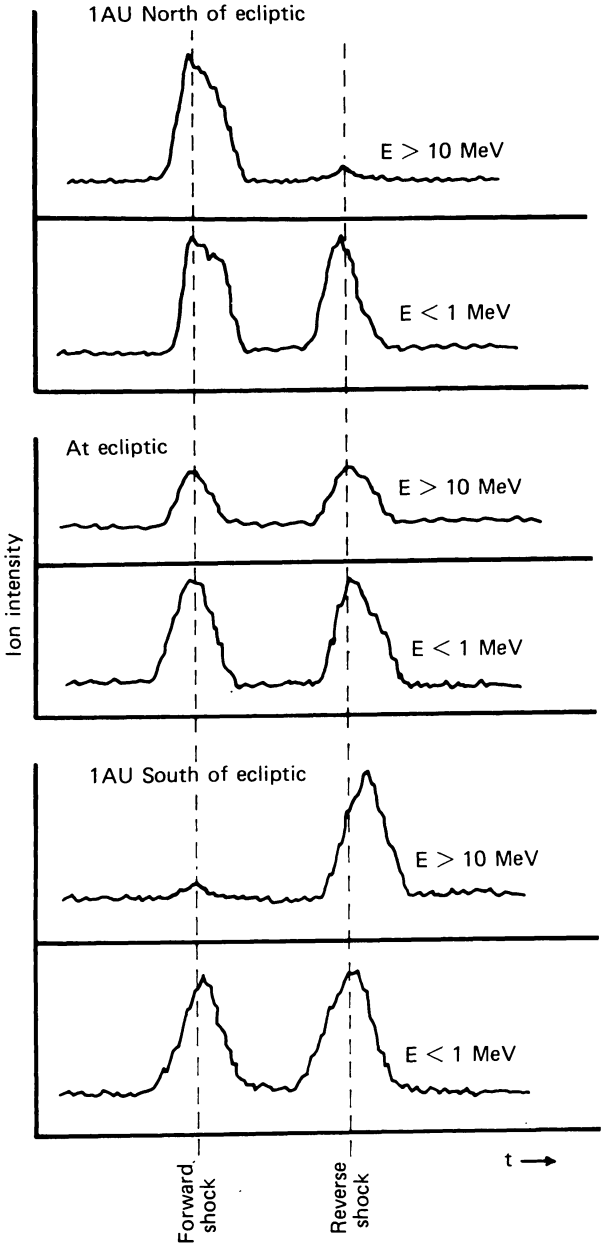


FIGURE 2. Anticipated particle intensity/time signatures for forward-reverse interplanetary shock pairs observed north of, south of, and in the ecliptic plane.

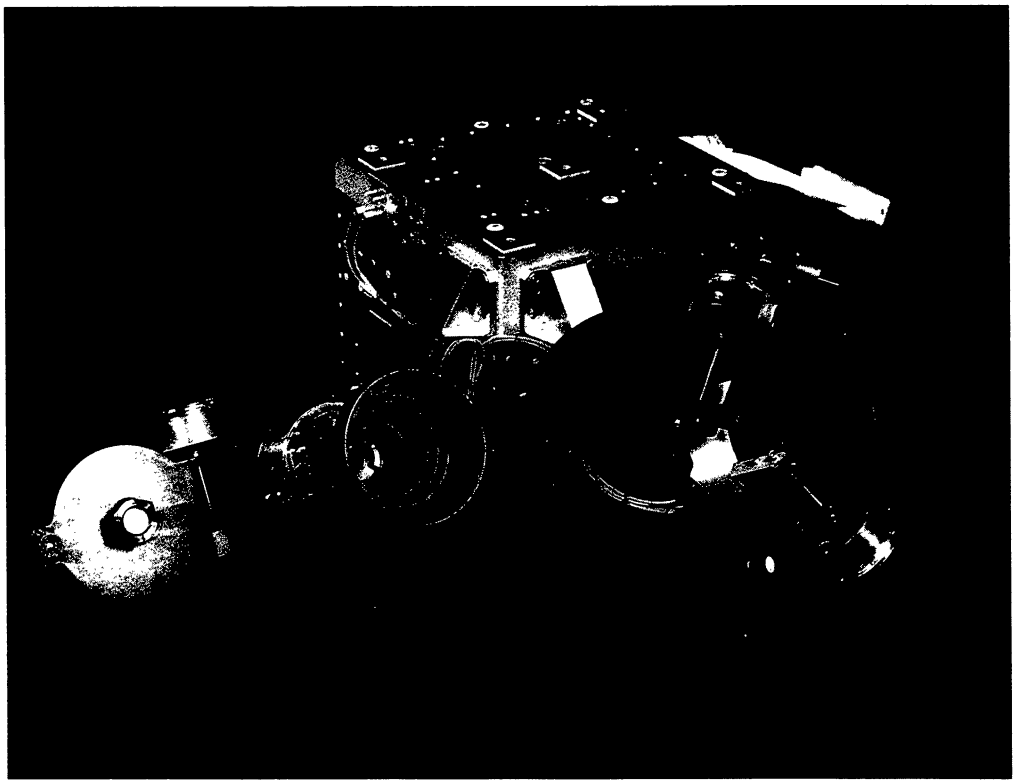

FIGURE 4a.

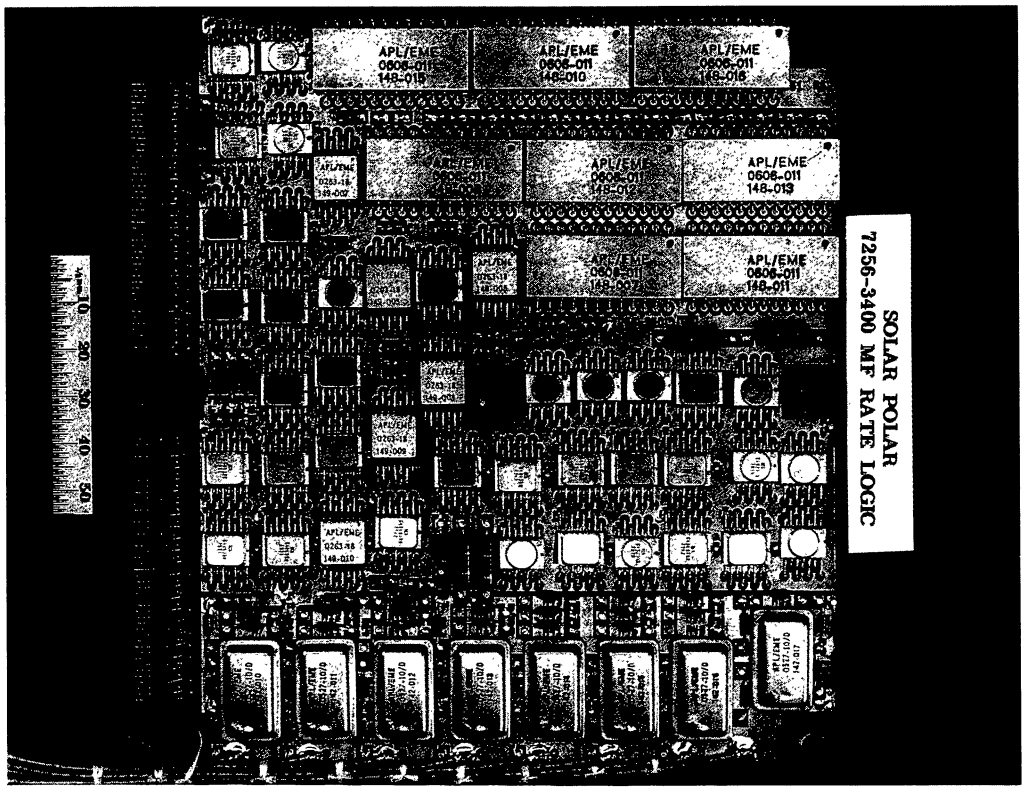


FIGURE 4b.

FIGURE 4. The HI-SCALE experiment: (a) Complete instrument assembly; (b) Circuit-board layout.

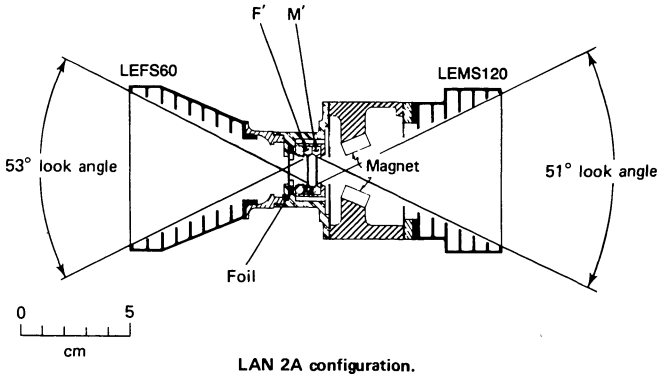


LAN 2A configuration.

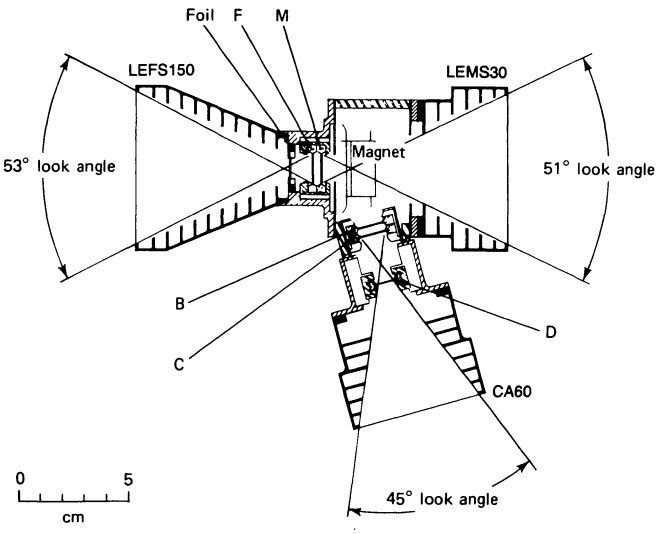


LAN 2B configuration.

FIGURE 5. Schematic outline of detector telescope configurations in the two separate mechanical mounts.

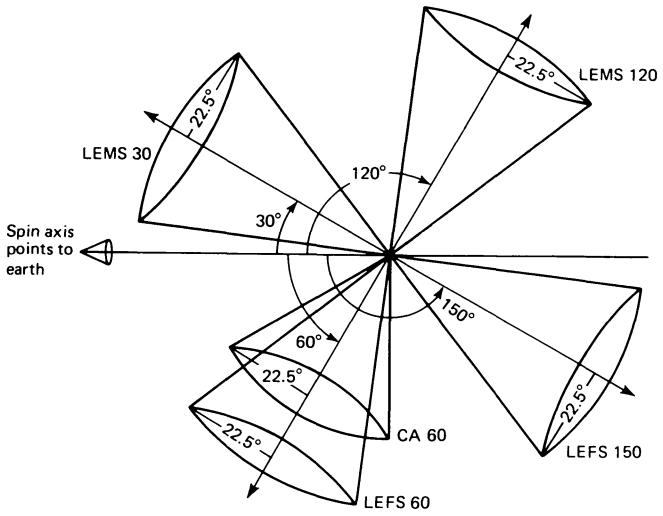


FIGURE 6a.

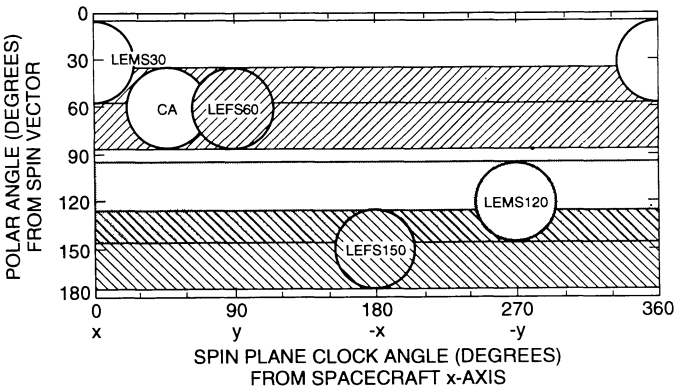


FIGURE 6b.

FIGURE 6. (a) Look angles of the five detector telescopes for the HI-SCALE experiment. (b) Instantaneous look direction of the four LEMS/LEFS telescopes on the $4\pi$ steradian sphere. One spacecraft rotation (~12s) takes each telescope through 360°, and thus the entire sphere is covered each rotation.

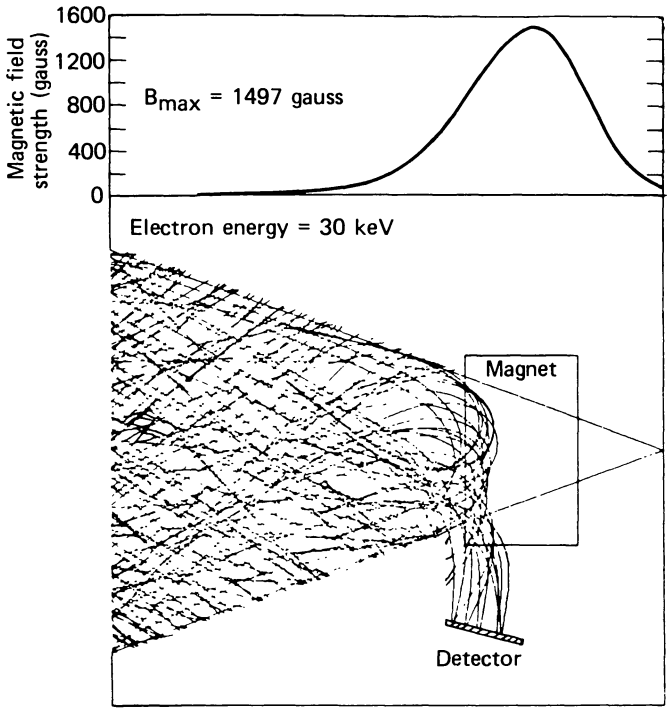


FIGURE 7. Example of electron trajectory ray tracing in a magnetic-field geometry similar to that used in the LEMS 30 HI-SCALE telescope.

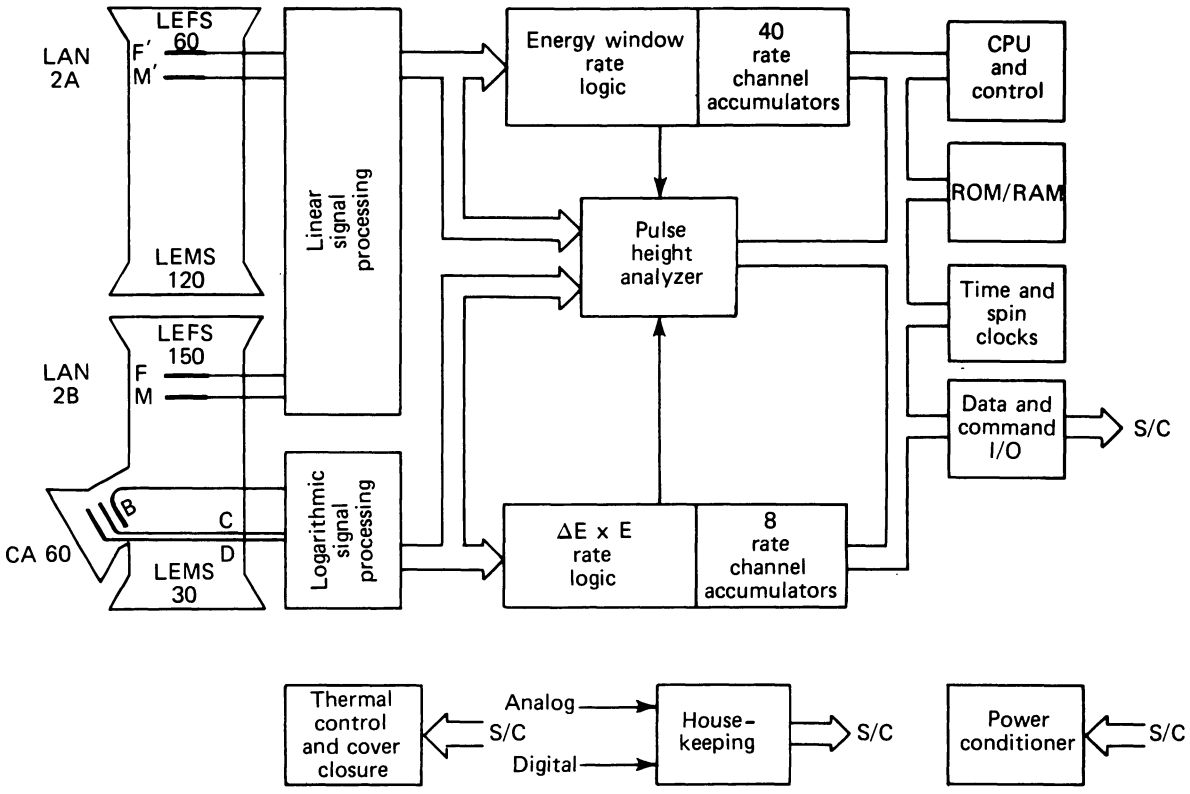


FIGURE 8. Block diagram of electronics system for the HI-SCALE experiment.

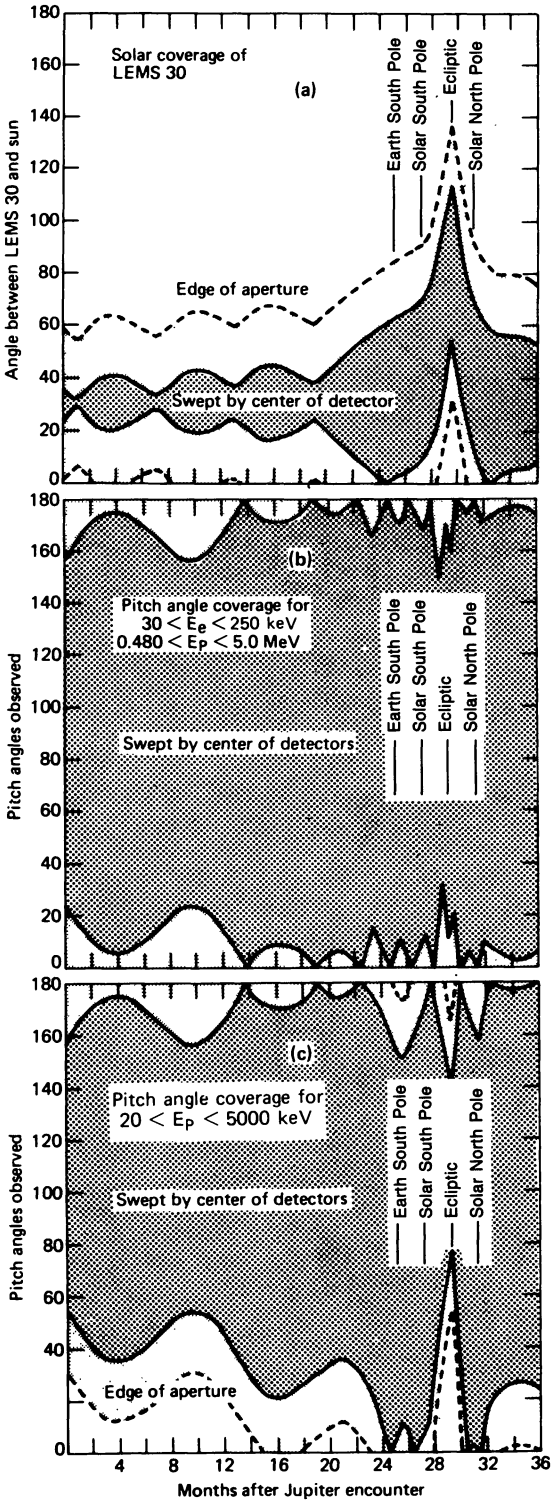


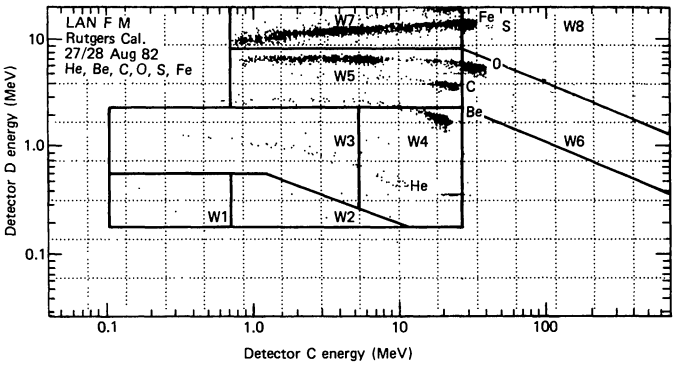


FIGURE 10a.

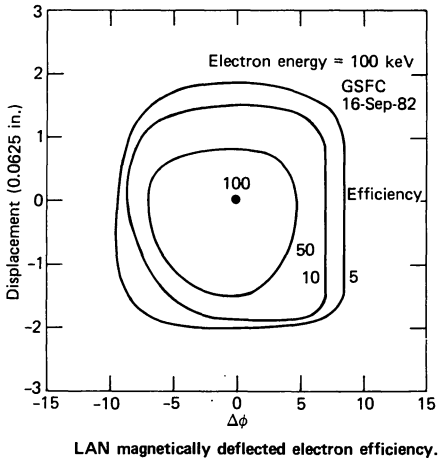


FIGURE 10b.

FIGURE 9. Pitch-angle coverage of selected electron and proton energies throughout the prime phase of the mission, out of the ecliptic plane, after Jupiter encounter. The pitch angles were determined assuming a nominal Archimedean spiral interplanetary magnetic field.

FIGURE 10. Calibration data: a) Energy-loss matrix for the composition aperture for various incident ions. The solid lines outline the discrete element groups detected (Tab. 3). b) Efficiency contours across the telescope aperture for detecting 100 keV electrons in the B detector.

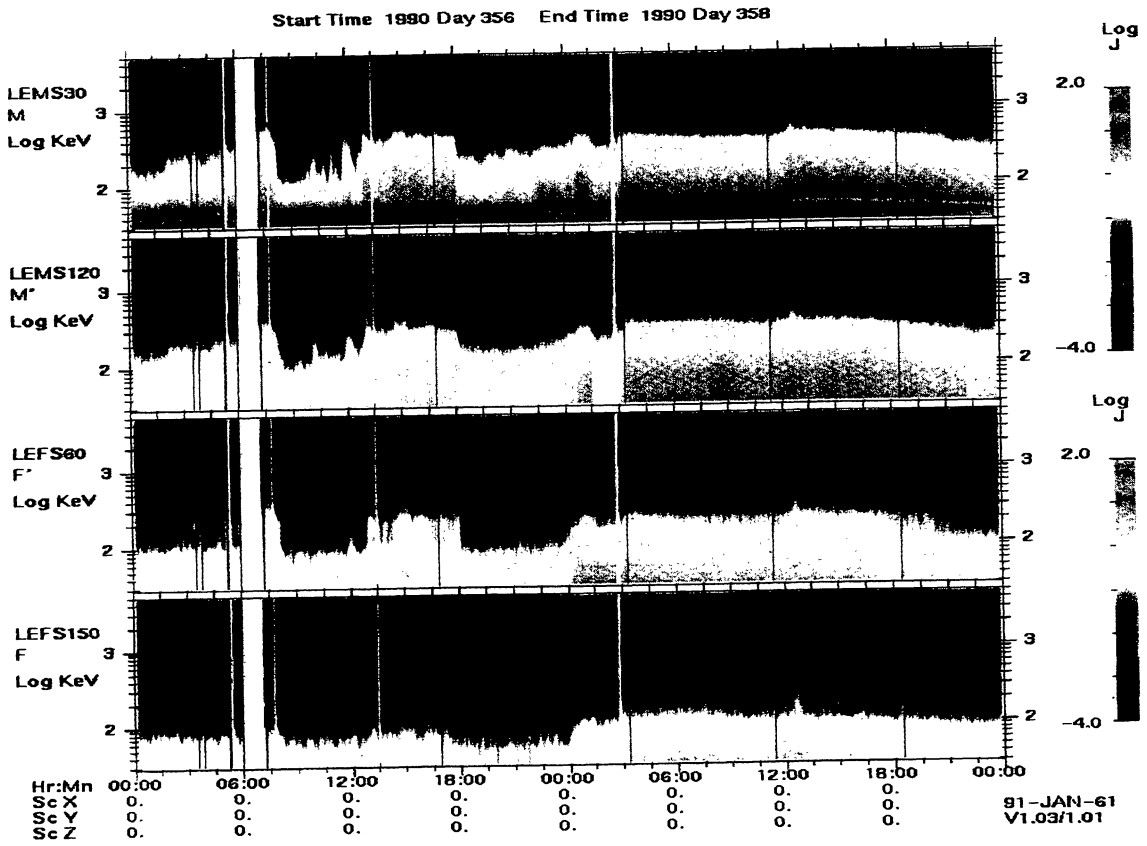


FIGURE 11. Time-intensity spectrograms of the ion intensities measured by the HI-SCALE instrument on days 356-357, 1990.

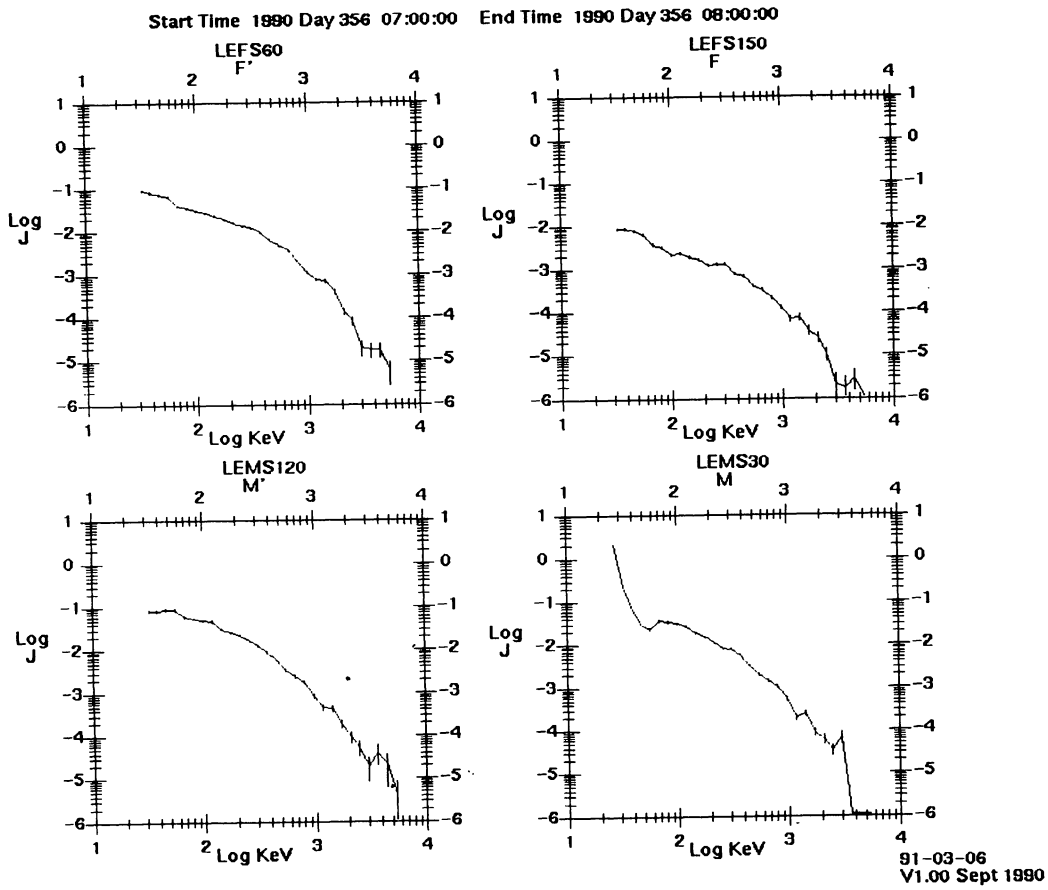


FIGURE 12. Ion spectra determined from the 32 rate channel accumulators for an one hour interval on day 356. The dimensions of the flux J are particles/(cm$^2$ sec sr keV).

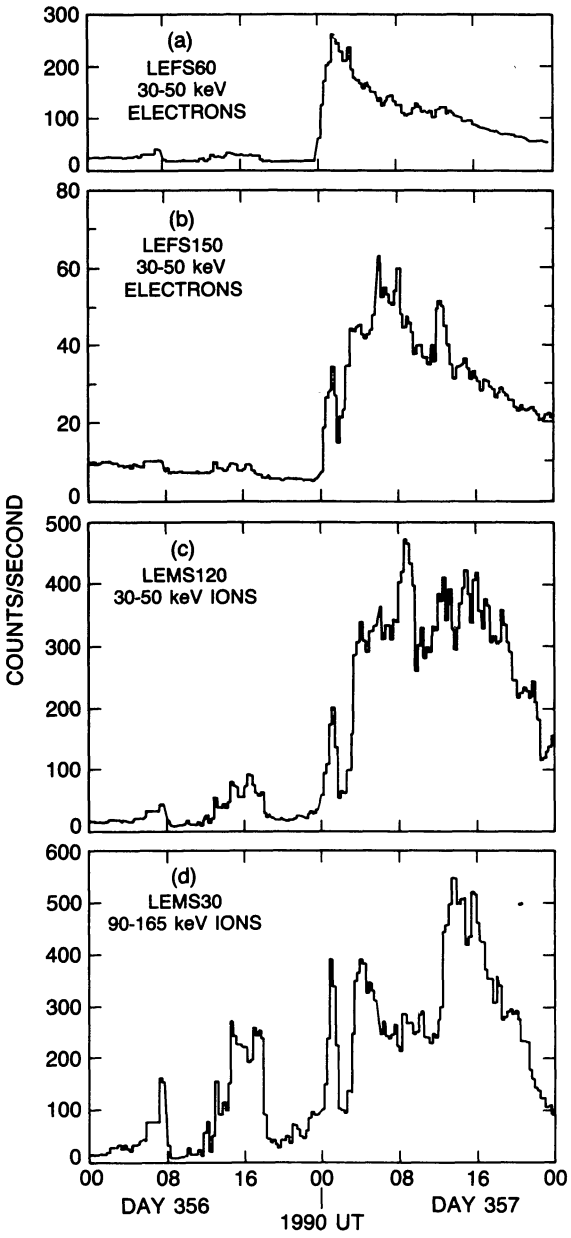


FIGURE 13. Time-intensity counting rate plots of selected particle and energy channels from the spectrum analyzer for days 356-357, 1990.

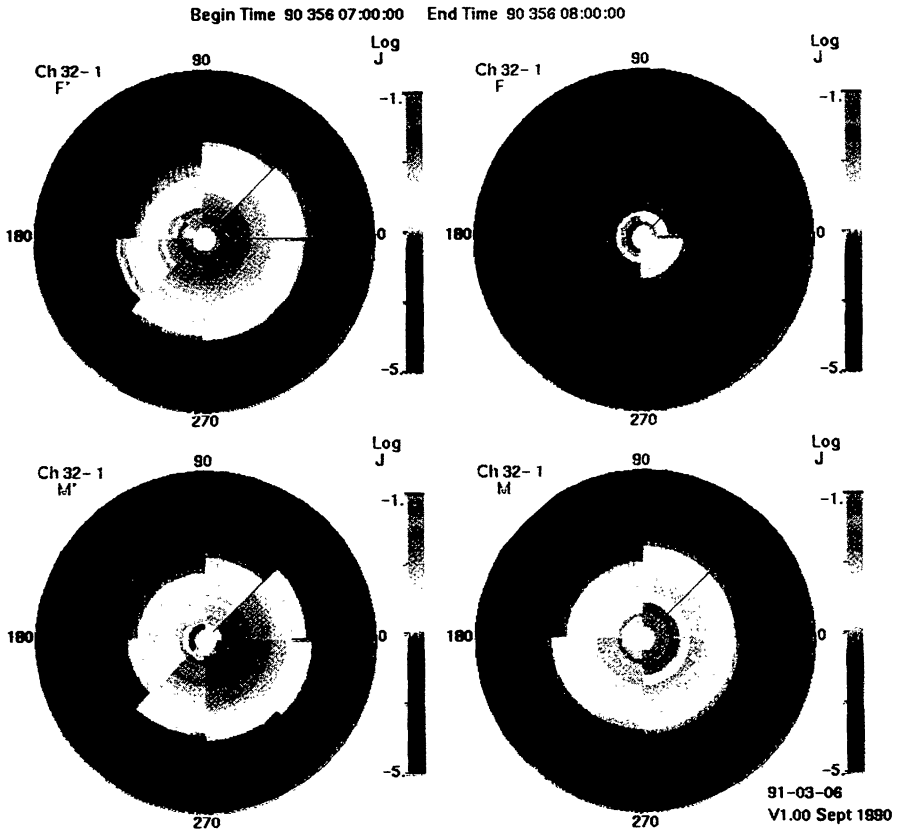


FIGURE 14. Ion spectra plotted as function of angular distribution to illustrate the angular sectoring of the HI-SCALE instrument. The intense low energy fluxes in the M detector are due to sunlight.

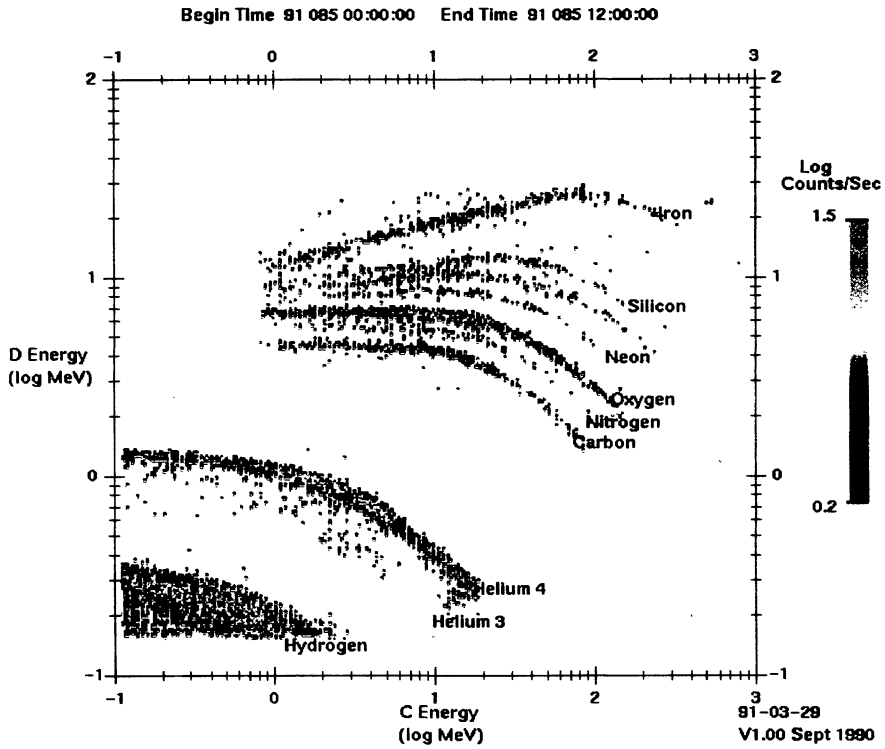


FIGURE 15. Ion flux composition matrix measured by the CA detector system during the first half of day 85, 1991. This interval occurred during a large solar particle event which swept over Ulysses at the end of March 1991.